Journal of Nuclear Materials 543 (2021) 152636

Contents lists available at ScienceDirect

Journal of Nuclear Materials

journal homepage: www.elsevier.com/locate/jnucmat

Void shrinkage in 21Cr32Ni austenitic model alloy during in-situ ion irradiation

M. Ayanoglu*, A.T. Motta

Ken and Mary Alice Lindquist Department of Nuclear Engineering, The Pennsylvania State University, University Park, PA, 16802, USA

ARTICLE INFO

Article history:
Received 7 September 2020
Revised 20 October 2020
Accepted 23 October 2020
Available online 31 October 2020

Keywords:
In-situ irradiation
void shrinkage
radiation damage
transmission electron microscopy
Fe-Cr-Ni
Fe21Cr32Ni
800H

ABSTRACT

Austenitic 21Cr32Ni model alloy thin foils, previously irradiated with 5 MeV Fe^{++} ions in bulk to create voids, were re-irradiated in-situ in the Intermediate Voltage Electron Microscope Facility (IVEM). The voids which had been formed under bulk-ion irradiation shrank and disappeared after in-situ Kr ion irradiation in the temperature range 50 K-713 K to an additional dose of 1 dpa. The voids were unaffected by eithersuccessive thermal annealing to 673 K and by prolonged exposure to the 200 keV electron beam at the irradiation temperature. The high void shrinkage rate observed did not change significantly for irradiation temperatures between 50 K and 713 K, suggesting that the void shrinkage process in thin foils during in-situ heavy-ion irradiation results from the interactions of displacement cascades with the voids. Possible void shrinkage mechanisms under thin foil irradiation are discussed in this study.

1. Introduction

The concern that excessive irradiation induced void swelling in stainless steels could occur in advanced nuclear reactors has led researchers to investigate void evolution under charged-particle irradiation using both in-situ and ex-situ transmission electron microscopy (TEM). The in-situ irradiation technique allows real-time observation of radiation-induced features formed under well-controlled conditions at a range of temperatures [1–15]. During in-situ irradiation experiments, void formation was only observed at relatively high irradiation doses (>20 dpa) and temperatures(>~825 K) [9]. On the other hand, during bulk-ion irradiation void formation was often observed in austenitic stainless steels after irradiation to much smaller doses (~1 dpa) at lower irradiation temperatures [16–22]. As a matter of fact, voids formed under neutron or bulk-ion irradiation have been observed to shrink when subjected to further in-situ electron or ion irradiation [4–8,23–29].

Laidler and Garner examined neutron-induced voids formed in annealed SS304 and SS316 type austenitic stainless-steel using high-voltage electron irradiation of 0.3-0.8 MeV at ~773 K and above [8,23]. They observed that voids located close to the foil surface shrank, while voids located in thicker regions of the foil (i.e. far from foil surface) were unaffected. Makin reported that neutron-induced voids in 316 type austenitic stainless steels shrink when irradiated in-situ at 973 K with 1 MeV electrons in the Harwell High Voltage Electron Microscope [24]. They attributed this effect to foil erosion during irradiation. A similar foil surface erosion was reported by Donnelly et al. who studied the effect of Xe ion impacts on the surfaces of fcc-Au using in-situ irradiation [25]. The authors reported the observation of the surface craters associated with expelled materials resultant from the ion impacts. The effect of foil surface on void shrinkage was further explored by Murphy using standard rate theory [26]. The author found that the void shrinkage time increases with decreasing foil thickness. This is because the foil surface becomes an increasingly effective defect sink for irradiation induced point defects relative to the cavities which results in increased defect loss to the foil surface. Singh and Foreman investigated void formation and growth in austenitic stainless steels under 1 MeV electron-irradiation at 973 K. In a small percentage of their experiments, they observed a few large voids initially increase in size but then rapidly shrink [27], while in other experiments they observed all voids to steadily grow. They reported that the shrinkage took place away from the foil surface and shrinkage rate was higher for voids attached to dislocations than for voids in the matrix, and attributed this difference to dislocation pipe-diffusion of interstitials [2,27]. A similar diffusion-pipe mechanism was suggested by Chen et al. [29]. The authors investigated void evolution in nanotwinned copper using in-situ ion irradiation of 1 MeV Kr^{++}. They observed that pre-existing

* Corresponding author.
E-mail address: ayanoglu.muhammed@gmail.com (M. Ayanoglu).

https://doi.org/10.1016/j.jnucmat.2020.152636
0022-3115/

Table 1
Bulk chemical composition of the major constituents of 21Cr32Ni model alloy measured by direct current plasma method.

Alloy	Fe	Ni	Cr	Mn	Al, Ti, V, Cu, Si, Mo, P, C*, S*)
21Cr32Ni	Bal.	31.2	20.7	0.9	<0.2

* Combustion method (CO) used for carbon and sulfur measurement.

voids at grain boundaries shrank after in-situ ion irradiation to ~1.56 dpa at room temperature. The shrinkage was attributed to pipe-diffusion of interstitials at grain boundaries, acting as faster diffusion channels for interstitials. When interstitials are absorbed at nanotwin grain boundaries, they immediately migrate to voids, causing shrinkage.

In a study conducted on the similar alloy 800H, Ulmer et al. observed that voids initially formed after 10 dpa bulk-ion irradiation at 713 K shrank after an additional 1-2 dpa in-situ irradiation with 1 MeV Kr^{++} at 713 K [7]. The authors found that the implanted interstitial concentration was too low to justify the observed void shrinkage and therefore, attributed to the shrinkage to the excess loss of mobile point defects (both vacancies and interstitials) to the foil surface which in turn reduces the vacancy concentration below the equilibrium vacancy concentration around voids, resulting in a net interstitial flux into the voids. The many different void shrinkage mechanisms in thin foils proposed in the literature, can be categorized into three classes: (1) net loss of vacancies from voids via thermal emission of vacancies during high temperature anneal [4]; (2) net interstitial gain to voids either by pipe-diffusion mechanism [2,29], by replacement collision sequences [30], by preferential interstitial absorption due to the stress field resultant from differential swelling [8,23], or by excess interstitial absorption due to the loss of vacancies to foil surface [7]; (3) other mechanisms such as gradual foil thinning, or foil surface erosion [24–25].

As it is seen, although these studies provide valuable data on void shrinkage observed under a variety of in-situ irradiation conditions, the proposed mechanisms of void shrinkage vary widely. Also, depending on the irradiation conditions, the void shrinkage time can vary from tens of minutes to tens of hours. In addition, void shrinkage during low temperature irradiation has not been investigated. Unfortunately, none of these mechanisms are applicable to the present case as discussed below.

In this paper, the mechanism of void shrinkage in a thin foil prepared from previously irradiated 21Cr32Ni austenitic model alloy was systematically investigated using in-situ Kr ion irradiation of performed at the Intermediate Voltage Electron Microscope (IVEM) facility at Argonne National Laboratory. This alloy is in essence a model of commercial alloy 800H - an advanced austenitic alloy proposed for next generation reactors which exhibits high corrosion and creep resistance [7]. The model alloy was initially bulk-ion irradiated using 5 MeV Fe^{++} ions to 1 dpa at 713 K in the Michigan Ion Beam Laboratory. Thin foils from these samples were prepared by FIB lift out and further irradiated using 1 MeV Kr^{++} ions with an additional dose of ~1 dpa in the temperature range 50 K-713 K using similar damage rates as were used during bulk-ion irradiation. The void diameter during irradiation was measured with respect to irradiation dose for various irradiation temperatures. The overall results are discussed in light of existing literature.

2. Experimental details

The 21Cr32Ni model alloy used in this study was provided by GE Global Research as heat #RAM-2192. The elemental composition of the alloys measured by Sherry Laboratories using direct current plasma (DCP) emission spectroscopy is shown in Table 1. The alloy grain size was determined by optical microscopy to be ~60 μm, after the polished surface was exposed to an etchant having a composition of 10 ml HNO_3, 20 ml HCl, and 30 ml H_2O.

Bulk-ion irradiation of 21Cr32Ni model alloy was performed at the Michigan Ion Beam Laboratory (MIBL). The 21Cr32Ni model alloy sample bar was irradiated to 1 dpa at 713 K (440°C) using 5 MeV Fe^{++} ions using a damage rate of 5×10^{-4} dpa/s. The corresponding iron ion flux is ~1.2×10^{12} ion/cm^2-s, to a total iron ion fluence is ~2.4×10^{15} ion/cm^2. TEM foils from the bulk-ion irradiated materials were prepared using focused ion beam (FIB) (shown in Fig. 1) performed with FEI Helios NanoLab660 using gallium (Ga^+) ions with 30kV, 5kV and 2kV final polishing steps with corresponding currents of 0.23 nA, 0.12 nA and 93 pA [16]. The damage profile of 5 MeV Fe^{++} ions was calculated using the Stopping and Range of Ion in Matter (SRIM) software [31] using the Quick Kinchin-Pease Model for displacement calculations and a displacement energy of 40 eV [16]. As indicated in Fig. 1 the depth at which the target dose was achieved is ~0.6 μm, to minimize both surface effects and the effect of the injected interstitials close to the ion range. The maximum penetration depth of Ga^+ is ~10 nm which was illustrated with a thin layer on Fig. 1c. Because the slice imaged in TEM has been only exposed to the ion beam on front surface and very low ion beam current was used at the final polishing step, the damage by gallium was assumed to be negligible compared to that formed after 5 MeV Fe+$^+$. The TEM observations beyond the ion range also revealed little FIB induced damage. Also, diffraction patterns recorded from the damaged region showed that there was no pre-existing or radiation-induced precipitate in the bulk-ion irradiated 21Cr32Ni samples due to the low alloying element content of the alloy.

These FIB-prepared TEM foils were further irradiated in-situ at the Intermediate Voltage Electron Microscope (IVEM) Facility at Argonne National Laboratory using 1 MeV Kr^{++} ions and an ion flux of 2.84×10^{11} ions/cm^2-s at temperatures ranging from 50 K to 713 K to investigate the evolution of the pre-existing voids under further ion irradiation. The sample temperature was continuously monitored throughout the experiments using a thermocouple attached to the specimen cup. The irradiation temperature was kept within ±5 K of the target value during irradiation. Pre-existing voids were imaged in the TEM by tilting the sample to a weak beam diffraction condition and recording bright-field TEM images. An effort was made to record all TEM images during irradiation using the same magnification (~60,000x) so that results were directly comparable. The void diameter was measured from the inner ring of the dark fringe using under-focused bright-field images. The average void diameter ($\bar{D}$), and the corresponding error of the measurement were calculated as described in [7,16].

The damage in dpa during in-situ 1 MeV Kr^{++} ion irradiation was calculated using SRIM software in the same manner as above. The ion flux during the in-situ irradiation was adjusted to give a damage rate of (5-10) $\times 10^{-4}$ dpa/s, similar to that obtained in bulk-ion irradiation at the specified depth (~0.6 μm). The calculation indicates that the vast majority of the Kr ions is transmitted through the thin foil; and only about ~3% of the incident ions are implanted. The thicknesses of the FIB samples were determined to be between ~80-100 nm using Convergent Beam Electron Diffraction (CBED) and confirmed by Energy Filtered Transmission Electron Microscopy (EFTEM) using an inelastic electron mean free path of ~110 nm [9,16].

3. Results

3.1. Pre-existing void structure in 21Cr32Ni model alloy after bulk-ion irradiation

Fig. 2 shows bright-field TEM images taken in under-focused conditions showing the initial void microstructure after 1 dpa bulk-

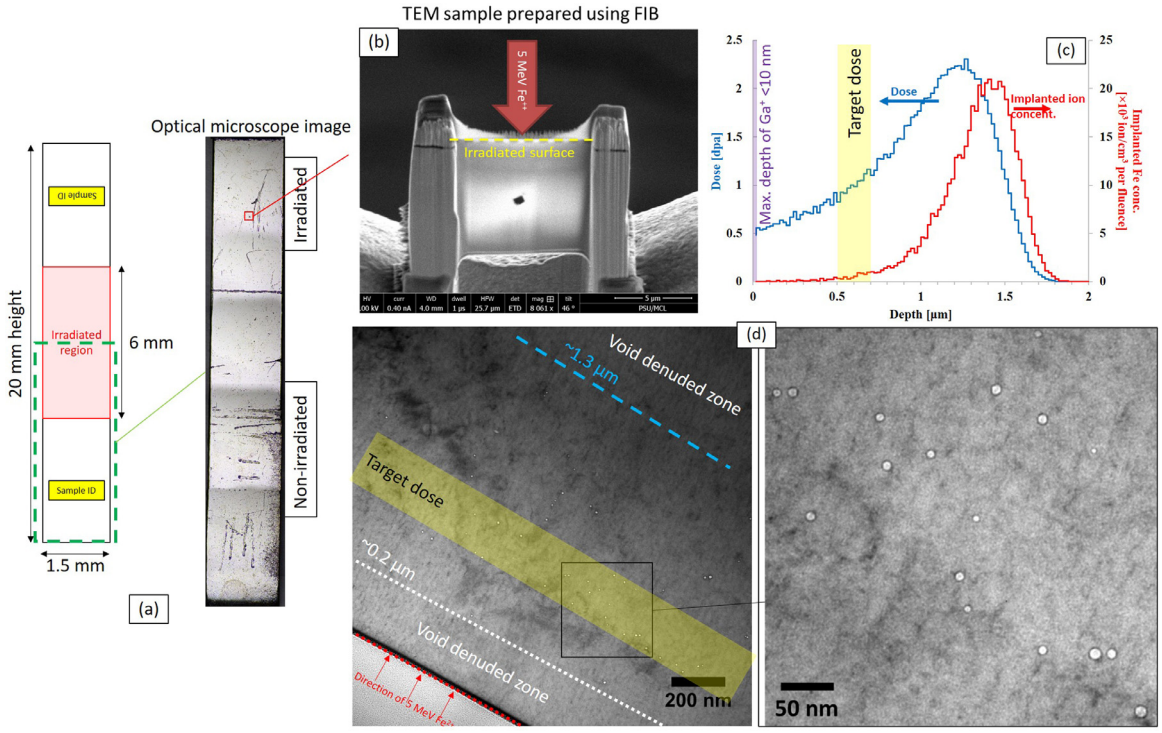

Fig. 1. (a) Schematic illustration of 1.5 mm thick 21Cr32Ni model alloy bar with the optical microscope image showing half of the bar used in bulk-ion irradiation, (b) TEM sample prepared from bulk-ion irradiated material, (c) The SRIM calculated damage and implanted Fe concentration profiles of 5 MeV Fe^{++} in 21Cr32Ni model alloy showing the depth at which the target dose is achieved. The maximum Ga^{+} depth from FIB sample preparation in 21Cr32Ni target is less than 10 nm and illustrated with purple color, (d) Bright-field TEM image showing the cross-section of FIB sample and void distribution. A denuded zone is observed near the irradiated surface (<~0.2 μm) and beyond ~1.3 μm. The voids in the target dose regionindicated with the black box are magnified in the last micrograph.

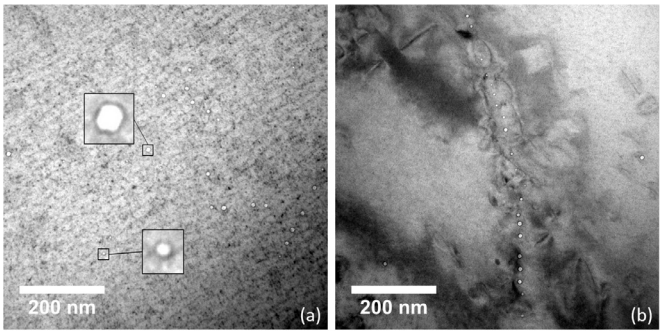

Fig. 2. Bright-field under-focused TEM image showing the void microstructure observed in 21Cr32Ni model alloy after bulk-ion irradiation to 1 dpa at 713 K. Voids were observed to be faceted and spherical as highlighted in Fig. 2a, and they are often found on pre-existing dislocations (Fig. 2b). (The contrast seen in the background in (a) is generated by radiation-induced aligned defect structures.)

ion irradiation of 21Cr32Ni model alloy at 713 K. Large voids (>8 nm) were either faceted (along the {111}-direction) or spherical (see magnified void images in Fig. 2). Relatively, smaller voids (<5 nm) were spherical.

During bulk-ion irradiation void formation often occurred preferentially at defect sinks, such as pre-existing dislocations or radiation-induced dislocation loops (see Fig. 2b as an example). The average void diameter in the irradiated foils was ~7-9 nm with a corresponding void number density on the order of ~5 × 10^{20} void/m^3. The maximum void diameter was ~9-11 nm. We note that after irradiation a denuded defect zone (no voids, no loops) – about ~0.2 μm wide– was consistently observed near the surface of the bulk irradiated samples.

3.2. Thermal annealing without irradiation

To study the thermal stability of the pre-existing voids in the 21Cr32Ni samples prior to in-situ ion irradiation, an annealing experiment was performed. Starting at 373 K, a 21Cr32Ni TEM foil sample that was ion-irradiated to 1 dpa at 713 K and which contained voids, was annealed for ~30 minutes, for each 100 K interval up to 673 K, with the electron beam was off. Bright-field images were acquired every 5 minutes. The total annealing time was ~130 minutes i.e., more than the total irradiation time required to reach ~1 dpa during in-situ ion irradiation (which is ~ 30 minutes at a damage rate of ~1 × 10^{-3} dpa/s).

The result of this annealing experiment is summarized in Fig. 3. The figure clearly shows that the initial void microstructure at room temperature is unaffected after successive 30 minute stages of thermal annealing up to 673 K suggesting that thermal vacancy emission from voids is negligible in this temperature range.

3.3. Void behavior under in-situ ion irradiation

When the samples were Kr ion irradiated in-situ in temperature range 50-713 K, all observed pre-existing voids shrank. Fig. 4 shows a series of under-focused bright-field TEM images that captures void shrinkage during additional in-situ ion irradiation at the two extreme irradiation temperatures used in this study: 50 K and 713 K. The majority of the pre-existing voids disappear after an additional in-situ irradiation dose of 0.4 dpa, and by 1 dpa total additional dose all voids disappear. It should be noted that no foil contrast difference or crater formation was observed during irradiation which indicates that ion induced foil sputtering or erosion was not a factor [24–25,32]. The results of the previous section indicate that thermal vacancy emission has negligible effect on void shrinkage. Thus, the observed void shrinkage in 21Cr32Ni model

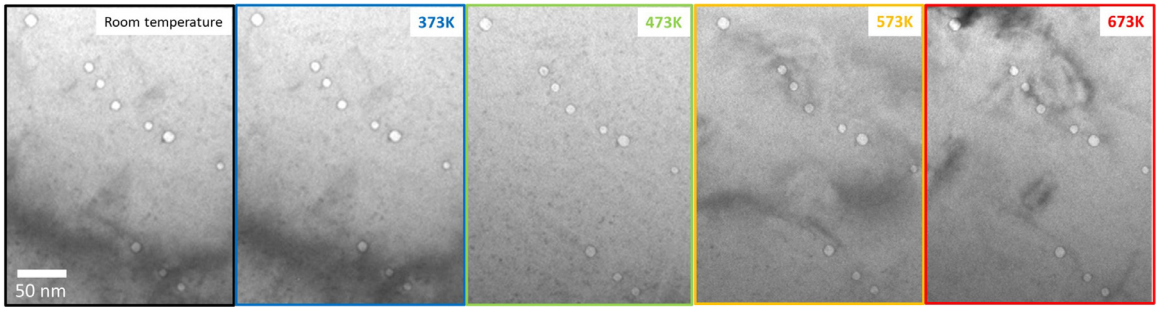

Fig. 3. Bright-field under-focused TEM images showing that pre-existing voids in 21Cr32Ni model alloy do not change after thermal annealing up to 673 K. The images were captured after ~30 minute anneals at the temperatures indicated.

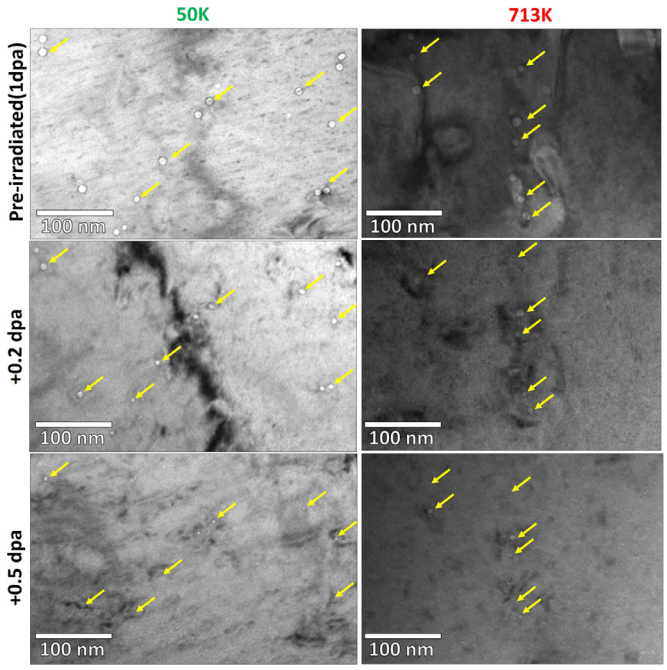

Fig. 4. Bright-field TEM images showing void shrinkage during in-situ irradiation of 1 dpa pre-irradiated 21Cr32Ni model alloy at 50 K and at 713 K and after additional 0.2 and 0.5 dpa Kr ion irradiation. Some of the voids are highlighted with yellow arrows at each dose to show void shrinkage and their subsequent disappearance. "Pre-irradiated" microstructures correspond to the microstructures after 1 dpa bulk-ion irradiation, whereas additional in-situ irradiation dose given to the pre-irradiated samples is shown as +dpa.

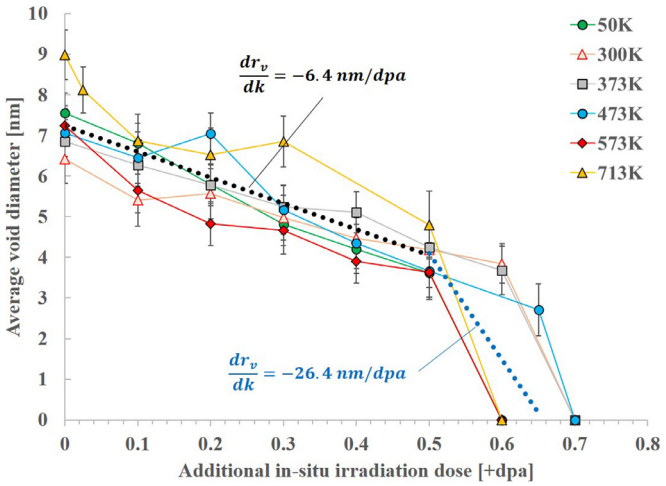

Fig. 5. Average void diameter in 21Cr32Ni model alloy as a function of irradiation dose and temperature.

alloy is caused by the displacement damage induced by in-situ ion irradiation.

To investigate the effect of irradiation temperature on void shrinkage, the average void diameter was measured as a function of irradiation dose and temperature. Fig. 5 shows the average void diameter from all the visible voids obtained from these measurements. The voids shrink at approximately the same rates at all irradiation temperatures, starting at an approximate rate of 6.4 nm/dpa when the void diameter decreases from 7 to 5 nm between 0 and 0.3 dpa, increasing to 26.4 nm/dpa in the last 0.1 dpa when the void size decreases below 3 nm, because of the higher surface to volume ratio in the smaller voids. We should note that per dpa the volume change in the void is 3 times higher in the first regime than in the second. The irradiation temperature does not have a noticeable effect on the void shrinkage rate between 50 K and 713 K.

To explore the shrinkage process further, a series of TEM snapshots of a pre-existing large void was analyzed at different stages of its shrinkage during in-situ irradiation at 473 K (see Fig. 6).

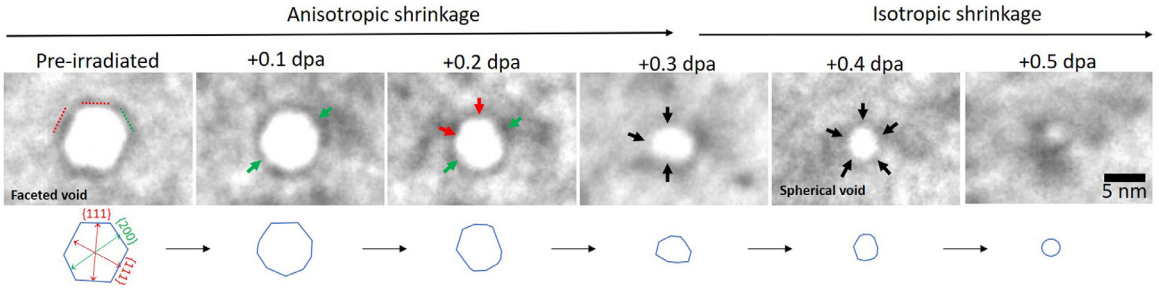

Fig. 6. Bright-field TEM images showing the evolution of an initially faceted void (schematic illustration is shown at the bottom) shrinking during in-situ ion irradiation at 473 K. The shrinkage direction is indicated with arrows on each image. Additional in-situ irradiation doses are shown as +dpa at the top of each image.

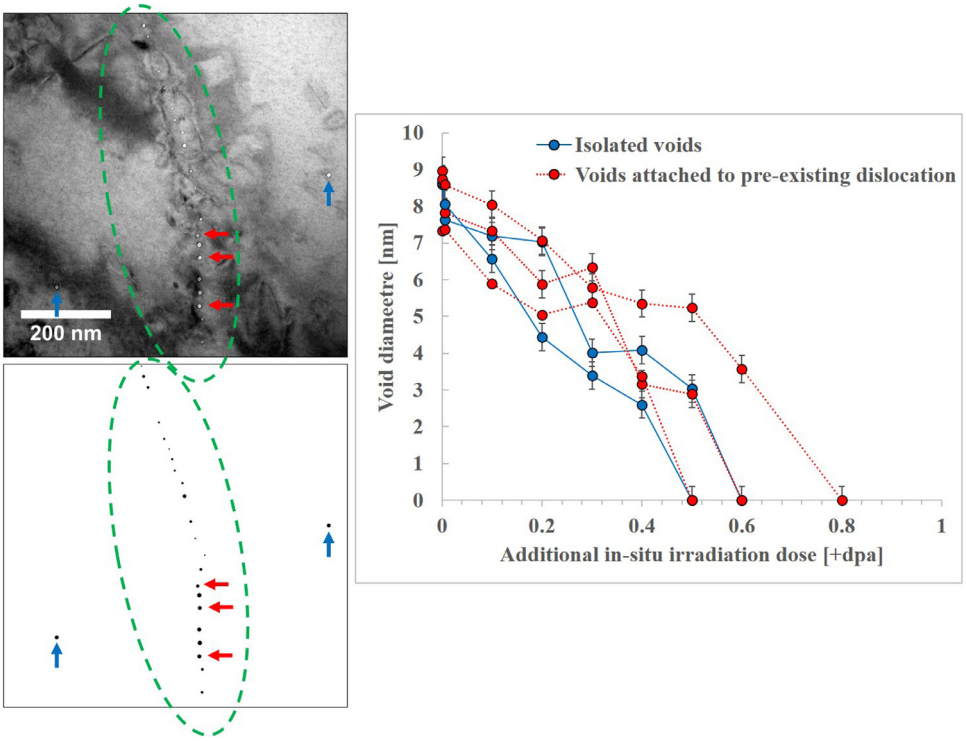

Fig. 7. Bright-field TEM image showing pre-existing voids formed in 21Cr32Ni model alloy after 1 dpa bulk Fe ion irradiation. The green dashed line highlights aligned voids which were preferentially formed on a pre-existing dislocation, while blue arrows indicate isolated voids. The plot on the right shows the shrinkage curves determined during in-situ Kr ion irradiation for of the individual voids indicated with red and blue arrows on the left.

Note that the initially faceted void becomes more spherical as it shrinks. No evidence was found that the pre-existing microstructure strongly influences the void shrinkage rate. Fig. 7 shows the void diameter vs. dose measured for the voids formed at dislocations and for isolated voids in the matrix. No meaningful difference in shrinkage rate is seen between the two types of voids.

Previous thermal annealing studies suggested that 200 keV electrons can accelerate void shrinkage [4]. Therefore, when irradiation was paused, voids away from the e-beam were checked, and they were found to have shrunk at the same rate as those that were being followed during irradiation. This is shown in Fig. 8 where the void shrinkage was captured in regions under the e-beam and away from the e-beam during the in-situ irradiation of 21Cr32Ni model alloy at 473 K. Fig. 9 shows quantitatively the that the void shrinkage rate under the e-beam and away from the e-beam are the same, which means that the processes leading to void shrinkage result from in-situ ion irradiation, and not from exposure to the electron beam.

4. Discussion

In this study, bulk Fe^{+} ion irradiation produced pre-existing voids in 21Cr32Ni model alloy shrank after in-situ thin foil Kr^{++}irradiation to 1 dpa in between 50 K-713 K. The net interstitial flux absorbed by the voids during the shrinkage ($N_{i,net}^{shrinkage}$) can be calculated from [7]:

$$N_{i,net}^{shrinkage} = \frac{\pi\left(d_f^3 - d_i^3\right)}{6\Omega\Delta t}$$

where d_i and d_f are the cavity diameter at the initial and final dose points and Ω is the atomic volume and taken to be ~10^{-23} cm^3 [33]. The average void shrinkage rate $N_{i,net}^{shrinkage}$ was calculated as a time average for more than ~200 voids. The result of this calculation showed that the net interstitial flux absorbed by the voids during the shrinkage was $N_{i,net}^{shrinkage}$ approximately *26 interstitial/s per void* which is consistent with the value previously reported of 22 interstitial/s per void for the analogue alloy 800H in-situ irradiated at 713 K [7].

The irradiation time for void shrinkage for the observed voids was ~15-20 minutes (corresponding to an additional dose of ~+1 dpa). This time is much shorter than that observed in previous thermal annealing studies and as well as electron irradiation studies performed in pure aluminum, and stainless steels using similar damage rates [4,8,34]. The latter observation suggests that individual displacement events are less effective than displacement cascades at causing void shrinkage.

Many possible explanations for shrinkage can be eliminated. If many ions are implanted, they could provide the additional interstitials to make the voids shrink. However, although ion implantation is a little higher in the thin foil irradiation conducted than in the bulk-ion irradiation this is not sufficient to explain the results [7]. Because no foil thinning [24] or crater formation [25] was observed, we also rule out the possibility of foil erosion as the cause of void shrinkage. A. Monterrosa et al. reported that the formation of M_2X-type carbide precipitates in dual-beam ion irradiated ferritic/martensitic T91 steels to 450 dpa at 733 K can suppress void swelling because they may act as point defect sinks [35]. However, no radiation-induced precipitation was observed in any of samples before or after the in-situ ion irradiation as was verified by the diffraction patterns recorded throughout the in-situ ion irradiation. In addition, considering the fact that void shrinkage was also observed even at 50 K where precipitate formation is not expected due to low defect mobility, the void shrinkage in 21Cr32Ni model alloy is not due to the formation of precipitates. Fig. 7 and Fig. 8 show that neither the pre-existing dislocation or grain microstructure nor the electron beam have a noticeable effect on the void shrinkage rates during in-situ ion irradiation. Thus, mechanisms of dislocation-pipe-diffusion or enhanced radiation diffusion

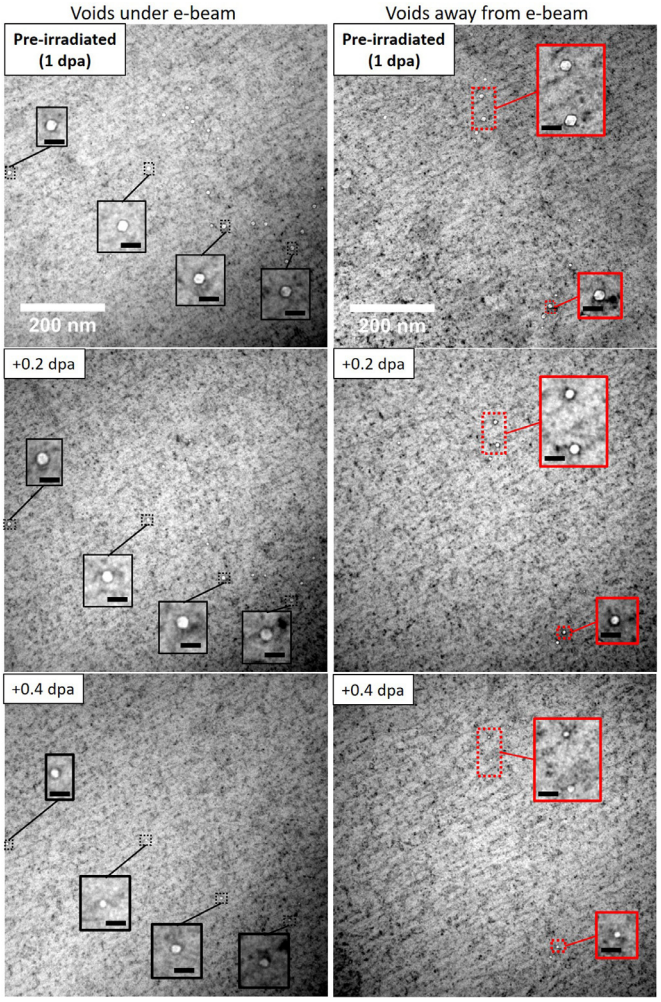

Fig. 8. Bright-field under-focused TEM images showing similar shrinkage of pre-existing voids both when under the 200 keV electron beam in the microscope and away from it, during 473 K in-situ ion irradiation. Both conditions yield the same shrinkage rate. (The contrast seen in the background are radiation-induced aligned defect structures). Scale bars in high magnification images (colored black) correspond to 20 nm. "Pre-irradiated" microstructures correspond to the microstructures after 1 dpa bulk-ion irradiation, whereas additional in-situ irradiation dose given to the pre-irradiated samples is shown as +dpa.

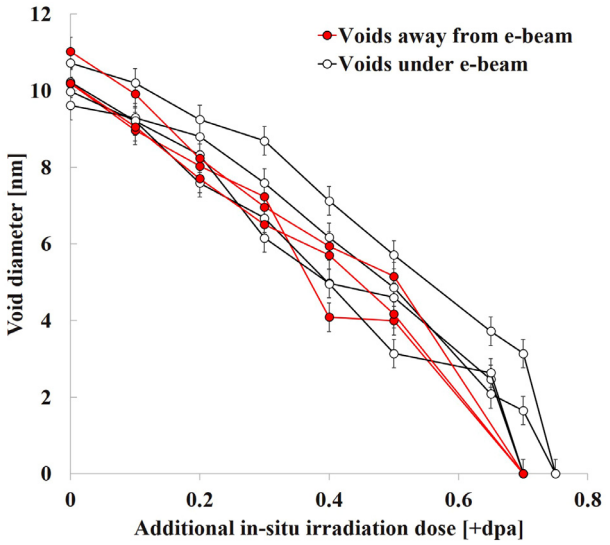

Fig. 9. Void diameter vs. dose during in-situ Kr ion irradiation for voids when irradiated under the 200 keV electron beam (white) and when irradiated away from the electron beam (red). The shrinkage rates are similar.

due to the electron beam are also not thought to be the driving forces leading to the rapid void shrinkage observed in this study.

It is clear that void shrinkage can only occur if there is a net vacancy flux from the void into the matrix or a net interstitial flux from the matrix to the void. Because our thermal annealing experiments showed no evidence of thermal vacancy emission in temperature range studied (50 K-713 K), void shrinkage is tentatively attributed to excess interstitial absorption by the voids during irradiation. The question is then posed as to what is it that causes the net flux of interstitials to the voids ($J_i^{void} - J_v^{void}$) to be *negative* during bulk irradiation and *positive* during thin foil irradiation. Although several results indicate that free surfaces affect void stability (as mentioned above, a void denuded zone is observed during bulk-ion irradiation, as also observed by other researchers [7,23]), the mechanism whereby this occurs is not clear.

One possibility to explain void shrinkage in thin foil irradiation is that radiation-induced vacancies migrate faster than interstitials and are lost to the foil surface (the dominant sink in thin foil irradiation) at a greater rate than interstitials. This would leave a higher fraction of interstitials in the foil which would be absorbed at the voids. However, this requires that the migration energy of vacancies be smaller than the migration energy of interstitials, which is not normally the case in metallic alloys [36]. In addition, Fig. 5 shows that the shrinkage process is independent from the irradiation temperature, which suggests that the process is not primarily driven by defect diffusion.

Recent molecular dynamics studies of displacement cascades in tungsten suggest that the diameter of pre-existing voids can decrease as a result of an interaction with an ion induced displacement cascade formed nearby [37]. This mechanism was also proposed by Agarwal et. al [38], who examined thin films of Fe containing pre-existing porosities/cavities (~2 nm), irradiated with 2 MeV Fe^{2+} to peak doses of 0.006 and 0.06 dpa at room temperature. After irradiation the films were examined using positron annihilation spectroscopy (PAS) and TEM. TEM analysis showed that the visible cavity number density is unchanged, but that the cavity diameter decreased with increasing dose. PAS analysis suggested an increase in the number density of very small vacancy clusters in the films. The authors explained the void shrinkage through an inward flux of interstitials created near the rim of a displacement cascade occurring near a void. The corresponding vacancies would then accumulate in the lattice, either as single defects or small clusters, increasing the invisible vacancy cluster density, in agreement with their PAS measurements. On the other hand, this mechanism should also occur during bulk irradiation and cause void shrinkage, whereas this study finds that voids *grow* under bulk-ion irradiation.

In a previous paper it was suggested that because the surface acts as a sink for defects, the defect concentrations are suppressed during thin foil irradiation relative to bulk irradiation, if both interstitials and vacancies are mobile enough to reach the surface [7]. In that circumstance, the vacancy concentration is decreased below the equilibrium vacancy concentration under irradiation around the cavities such that there is negligible absorption of vacancies, or possibly some emission of vacancies from the void. This process would occur only under irradiation, as observed. It is, however, unlikely that both defects are mobile at 50 K.

Although numerous mechanisms leading to void shrinkage have been suggested in the literature, none of them was sufficient to answer the main question of "*why do voids that are stable under bulk-ion irradiation become unstable and shrink under in-situ ion irradiation?*". The difference between the sample behavior during in-

situ and bulk irradiation is striking and should be explained so that material behavior under irradiation can be better understood.

5. Summary and Conclusion

Pre-existing voids formed during 5 MeV Fe^{++} bulk-ion irradiated 21Cr32Ni model alloy after 1 dpa at 713 K were investigated under 1 MeV Kr^{++} in-situ ion irradiation up to an additional 1 dpa in the temperature range of 50 K-713 K. The results are as follows:

1. In-situ ion irradiation caused pre-existing voids to shrink and disappear. This was observed only under in-situ ion irradiation. The voids remained stable during thermal annealing and under electron-beam. Voids that had been preferentially formed along dislocations shrank at the same rates as other voids.
2. The rate of void shrinkage was the same at all irradiation temperatures from 50 K to 713 K. The fact that shrinkage occurs at 50 K suggest a displacement cascade-driven athermal process.
3. Several possibilities to explain this phenomenon are ruled out, including ion implantation, thin foil erosion and thermal vacancy emission. The exact mechanism for void shrinkage under think foil irradiation is not yet known.

Declaration of Competing Interest

None.

Acknowledgments

This work was supported by a DOE NEUP Integrated Research Project (IRP) by the U.S. Department of Energy under award number DE-NE0000639. We thank our collaborators at the Michigan Ion Beam Laboratory, Stephen Taller and Gary Was for the bulk sample irradiations. The authors would also like to thank Mark Kirk, Meimei Li, Ed Ryan, and Pete Baldo for their assistance on carrying out the in-situ ion irradiation experiments, and Djamel Kaoumi for his valuable comments.

References

[1] J.E. Harbottle, Philos. Mag. 27 (1973) 147–157.
[2] T.E. Volin, K.H. Lie, R.W. Balluffi, Act. Metal. 19 (1971) 263–274.
[3] T. Leffers, B.N. Singh, P. Barlow, in: Riso-M, Report No. 1937, Riso National Laboratory, Roskilde, Denmark, 1977, p. 38.
[4] Z. Zhang, et al., J. Appl. Cryst 49 (2016) 1459–1470.
[5] D.I.R. Norris, Nature 227 (1970) 830–831.
[6] Y.V. Konobeev, V.A. Pechenkin, F.A. Garner, in: ASTM STP 1366, American Society for Testing and Materials, 1998, pp. 699–712.
[7] C.J. Ulmer, A.T. Motta, J. Nucl, Mater 498 (2018) 458–467.
[8] J.J. Laidler, B. Mastel, F.A. Garner, in: ASTM STP 570, American Society for Testing and Materials, 1975, pp. 451–468.
[9] M. Desormeaux, A.T.Motta B.Rouxel, C.Bisor M.Kirk, Y. Carlan, A. Legrise, J. Nucl. Mater. 475 (2016) 156–167.
[10] C. Xu, W. Chen, Y. Chen, Y. Yang, J. Nucl. Mater. 509 (2018) 644–653.
[11] C. Xu, Y. Lu, Z. Fu, Y. Yang, J. Nucl. Mater. 529 (2020) 151911.
[12] R.W. Harrison, N. Peng, R.P. Webb, J.A. Hinks, S.E. Donnelly, Fusion Eng. Des 138 (2019) 210–216.
[13] D.J. Mazey, B.L. Eyre, J.H. Evans, J. Nucl. Mater. 64 (1977) 145–156.
[14] N.H. Packan, D.N. Braski, J. Nucl. Mater. 34 (1970) 307–314.
[15] J.E. Harbottle, S.F. Pugh, M.H. Loretto, D.I.R. Norris, Voids Formed By Irradiation of Reactor Materials (1971) 293–300 https://doi.org/10.1680/vfbiorm.44623.0026.
[16] M. Ayanoglu, A.T. Motta, J. Nucl. Mater. 510 (2018) 297–311.
[17] A.J.E. Foreman, Voids Formed by Irradiation of Reactor Materials„ in: Conference Proceedings, British Nuclear Energy Society, England, 1971, pp. 121–132.
[18] J. L.Straalsund, R.W. Powell, B.A. Chin, J. Nucl. Mater. 108–109 (1982) 299–305.
[19] B. Master, J.L. Brimhall, J. Nucl. Mater. 28 (1968) 115–117.
[20] J.L. Brimhall, B.J. Mastel, J. Nucl. Mater. 29 (1969) 123–125.
[21] J.A. Hudson, D.J. Mazey, R.S. Nelson, J. Nucl. Mater. 41 (1971) 241–256.
[22] D.J. Mazey, J.A. Hudson, R.S. Nelson, J. Nucl. Mater. 41 (1971) 257–273.
[23] F.A. Garner, J.J. Laidler, B. Mastel, L.E. Thomas, in: Properties of Reactor Structural Alloys after Neutron or Particle Irradiation, ASTM STP 570, American Society for Testing and Materials, 1975, pp. 433–448.
[24] M.J. Makin, J. Nucl. Mater. 71 (2) (1978) 300–308.
[25] S.E. Donnelly, R.C. Birtcher, Ion-induced spike effects on metal surfaces, Philosophical Magazine A 79 (1) (1999) 133–145, doi:10.1080/01418619908214279.
[26] S.M. Murphy, J. Nucl. Mater. 118 (1983) 121–124.
[27] B.N. Singh, A.J.E. Foreman, Void shrinkage in stainless steel during high energy electron irradiation, Risø National Laboratory, Roskilde, Denmark, 1976 Risø-M, No. 1845.
[28] D.I.R. Norris, Radiation Induced Voids in Metals, in: J.W. Corbett, L.C. Ianniello (Eds.), Proceedings of International Conference, CONF-710601, U.S. Atomic Energy Commission, 1971, p. 821.
[29] Y. Chen, K. Yu, Y Liu, et al., Damage-tolerant nanotwinned metals with nanovoids under radiation environments, Nat Commun 6 (2015) 7036 https://doi.org/10.1038/ncomms8036.
[30] R.S. Nelson, J. Nucl. Mater. 57 (1975) 77.
[31] J.F. Ziegler, J.P. Biersack, U. Littmark, The Stopping and Range of Ions in Solids, 1, Pergamon Press, Oxford, 1985 ed.
[32] Hinks, J. A., et al. "Effects of crystallographic and geometric orientation on ion beam sputtering of gold nanorods." Scientific reports 8.1 (2018): 1-10
[33] W. Coghlan, L. Mansur, J. Nucl. Mater. 122 (1984) 495–501.
[34] J. Zhang, F. Ma, Kei Xu, App. Surf. Sci. 229 (2004) 34–42.
[35] A. Monterrosa, D. Woodley, Z. Jiao, G. Was, J. Nucl. Mater. 509 (2018) 722–735.
[36] W.G. Wolfer, Comp. Nucl. Mat. 1 (2012) 1–45.
[37] A. Fellman, A.E. Sand, J. Byggmastar, K. Nordlund, J. Phys. Cond. Matter 31 (2019) 405402.
[38] S. Agarwal, et al., Sci. Adv. 6 (2020) 31, eaba8437.